intercellular adhesion molecule 1 and HLA class I and class II antigens in rheumatoid synovial fibroblasts. Arthritis Rheum 1990;33:1776–86.
5. Feldmann M, Brennan FM, Chantry D, Haworth C, Turner M, Abney E, et al. Cytokine production in the rheumatoid joint: implications for treatment. Ann Rheum Dis 1990;49:480–6.
6. Chu CQ, Field M, Feldmann M, Maini RN. Localization of tumor necrosis factor α in synovial tissues and at the cartilage–pannus junction in patients with rheumatoid arthritis. Arthritis Rheum 1991;34:1125–32.
7. Tak PP, Bresnihan B. The pathogenesis and prevention of joint damage in rheumatoid arthritis: advances from synovial biopsy and tissue analysis [review]. Arthritis Rheum 2000;43:2619–33.
8. Takayanagi H, Oda H, Yamamoto S, Kawaguchi H, Tanaka S, Nishikawa T, et al. A new mechanism of bone destruction in rheumatoid arthritis: synovial fibroblasts induce osteoclastogenesis. Biochem Biophys Res Commun 1997;240:279–86.
9. Zhang G, Ghosh S. Molecular mechanisms of NF-κB activation induced by bacterial lipopolysaccharide through Toll-like receptors. J Endotoxin Res 2000;6:453–7.
10. Choe JY, Crain B, Wu SR, Corr M. Interleukin 1 receptor dependence of serum transferred arthritis can be circumvented by toll-like receptor 4 signaling. J Exp Med 2003;197:537–42.
11. Bamba T, Kanauchi O, Andoh A, Fujiyama Y. A new prebiotic from germinated barley for nutraceutical treatment of ulcerative colitis. J Gastroenterol Hepatol 2002;17:818–24.
12. Inan MS, Rasoulpour RJ, Yin L, Hubbard AK, Rosenberg DW, Giardina C. The luminal short-chain fatty acid butyrate modulates NF-κB activity in a human colonic epithelial cell line. Gastroenterology 2000;118:724–34.
13. Weaver GA, Krause JA, Miller TL, Wolin MJ. Short chain fatty acid distributions of enema samples from a sigmoidoscopy population: an association of high acetate and low butyrate ratios with adenomatous polyps and colon cancer. Gut 1988;29:1539–43.
14. Kashtan H, Stern HS, Jenkins DJ, Jenkins AL, Thompson LU, Hay K, et al. Colonic fermentation and markers of colorectal-cancer risk. Am J Clin Nutr 1992;55:723–8.
15. Segain JP, Raingeard de la Bletiere D, Bourreille A, Leray V, Gervois N, Rosales C, et al. Butyrate inhibits inflammatory responses through NFκB inhibition: implications for Crohn's disease. Gut 2000;47:397–403.
16. Ahmad MS, Krishnan S, Ramakrishna BS, Mathan M, Pulimood AB, Murthy SN. Butyrate and glucose metabolism by colonocytes in experimental colitis in mice. Gut 2000;46:493–9.
17. Pazin MJ, Kadonaga JT. What's up and down with histone deacetylation and transcription? Cell 1997;89:325–8.
18. Espinos E, Le V, Thai A, Pomies C, Weber MJ. Cooperation between phosphorylation and acetylation processes in transcriptional control. Mol Cell Biol 1999;19:3474–84.
19. Atsumi T, Nishihira J, Makita Z, Koike T. Enhancement of oxidised low-density lipoprotein uptake by macrophages in response to macrophage migration inhibitory factor. Cytokine 2000; 12:1553–6.
20. Heid CA, Stevens J, Livak KJ, Williams PM. Real time quantitative PCR. Genome Res 1996;6:986–94.
21. Chen J, Amasaki Y, Kamogawa Y, Nagoya M, Arai N, Arai K, et al. Role of NFATx (NFAT4/NFATc3) in expression of immunoregulatory genes in murine peripheral CD4+ T cells. J Immunol 2003;170:3109–17.
22. Semon D, Kawashima E, Jongeneel CV, Shakhov AN, Nedospasov SA. Nucleotide sequence of the murine TNF locus, including the TNF-α (tumor necrosis factor) and TNF-β (lymphotoxin) genes. Nucleic Acids Res 1987;15:9083–4.
23. Ino T, Yasui H, Hirano M, Kurosawa Y. Identification of a member of the TIS11 early response gene family at the insertion point of a DNA fragment containing a gene for the T-cell receptor β chain in an acute T-cell leukemia. Oncogene 1995;11:2705–10.
24. Amasaki Y, Adachi S, Ishida Y, Iwata M, Arai N, Arai K, et al. A constitutively nuclear form of NFATx shows efficient transactivation activity and induces differentiation of CD4(+)CD8(+) T cells. J Biol Chem 2002;277:25640–8.
25. Van den Berg WB, van Lent PL. The role of macrophages in chronic arthritis. Immunobiology 1996;195:614–23.
26. McCarthy JE, Kollmus H. Cytoplasmic mRNA-protein interactions in eukaryotic gene expression. Trends Biochem Sci 1995;20: 191–7.
27. Xu N, Chen CY, Shyu AB. Modulation of the fate of cytoplasmic mRNA by AU-rich elements: key sequence features controlling mRNA deadenylation and decay. Mol Cell Biol 1997;17:4611–21.
28. Peng SS, Chen CY, Shyu AB. Functional characterization of a non-AUUUA AU-rich element from the c-jun proto-oncogene mRNA: evidence for a novel class of AU-rich elements. Mol Cell Biol 1996;16:1490–9.
29. Bakheet T, Frevel M, Williams BR, Greer W, Khabar KS. ARED: human AU-rich element-containing mRNA database reveals an unexpectedly diverse functional repertoire of encoded proteins. Nucleic Acids Res 2001;29:246–54.
30. Bakheet T, Williams BR, Khabar KS. ARED 2.0: an update of AU-rich element mRNA database. Nucleic Acids Res 2003;31: 421–3.
31. Carballo E, Lai WS, Blackshear PJ. Feedback inhibition of macrophage tumor necrosis factor-α production by tristetraprolin. Science 1998;281:1001–5.
32. Taylor GA, Carballo E, Lee DM, Lai WS, Thompson MJ, Patel DD, et al. A pathogenetic role for TNFα in the syndrome of cachexia, arthritis, and autoimmunity resulting from tristetraprolin (TTP) deficiency. Immunity 1996;4:445–54.
33. Carballo E, Gilkeson GS, Blackshear PJ. Bone marrow transplantation reproduces the tristetraprolin-deficiency syndrome in recombination activating gene-2 (−/−) mice: evidence that monocyte/macrophage progenitors may be responsible for TNFα overproduction. J Clin Invest 1997;100:986–95.
34. Phillips K, Kedersha N, Shen L, Blackshear PJ, Anderson P. Arthritis suppressor genes TIA-1 and TTP dampen the expression of tumor necrosis factor α, cyclooxygenase 2, and inflammatory arthritis. Proc Natl Acad Sci U S A 2004;101:2011–6.
35. Johnson BA, Geha M, Blackwell TK. Similar but distinct effects of the tristetraprolin/TIS11 immediate-early proteins on cell survival. Oncogene 2000;19:1657–64.
36. Varnum BC, Ma QF, Chi TH, Fletcher B, Herschman HR. The TIS11 primary response gene is a member of a gene family that encodes proteins with a highly conserved sequence containing an unusual Cys-His repeat. Mol Cell Biol 1991;11:1754–8.
37. Blackshear PJ. Tristetraprolin and other CCCH tandem zinc-finger proteins in the regulation of mRNA turnover. Biochem Soc Trans 2002;30:945–52.
38. Lai WS, Carballo E, Strum JR, Kennington EA, Phillips RS, Blackshear PJ. Evidence that tristetraprolin binds to AU-rich elements and promotes the deadenylation and destabilization of tumor necrosis factor α mRNA. Mol Cell Biol 1999;19: 4311–23.
39. Maclean KN, McKay IA, Bustin SA. Differential effects of sodium butyrate on the transcription of the human TIS11 family of early-response genes in colorectal cancer cells. Br J Biomed Sci 1998;55:184–91.
40. Stoecklin G, Colombi M, Raineri I, Leuenberger S, Mallaun M, Schmidlin M, et al. Functional cloning of BRF1, a regulator of ARE-dependent mRNA turnover. EMBO J 2002;21:4709–18.
41. Wang SW, Pawlowski J, Wathen ST, Kinney SD, Lichenstein HS, Manthey CL. Cytokine mRNA decay is accelerated by an inhibitor of p38-mitogen-activated protein kinase. Inflamm Res 1999;48:533–8.
42. Dean JL, Sully G, Clark AR, Saklatvala J. The involvement of AU-rich element-binding proteins in p38 mitogen-activated pro-

tein kinase pathway-mediated mRNA stabilisation. Cell Signal 2004;16:1113–21.
43. Mahtani KR, Brook M, Dean JL, Sully G, Saklatvala J, Clark AR. Mitogen-activated protein kinase p38 controls the expression and posttranslational modification of tristetraprolin, a regulator of tumor necrosis factor α mRNA stability. Mol Cell Biol 2001;21: 6461–9.
44. Tchen CR, Brook M, Saklatvala J, Clark AR. The stability of tristetraprolin mRNA is regulated by mitogen-activated protein kinase p38 and by tristetraprolin itself. J Biol Chem 2004;279: 32393–400.
45. Brooks SA, Connolly JE, Rigby WF. The role of mRNA turnover in the regulation of tristetraprolin expression: evidence for an extracellular signal-regulated kinase-specific, AU-rich element-dependent, autoregulatory pathway. J Immunol 2004;172:7263–71.
46. Daniel C, Schroder O, Zahn N, Gaschott T, Stein J. p38 MAPK signaling pathway is involved in butyrate-induced vitamin D receptor expression. Biochem Biophys Res Commun 2004;324: 1220–6.
47. Venkatraman A, Ramakrishna BS, Shaji RV, Kumar NS, Pulimood A, Patra S. Amelioration of dextran sulfate colitis by butyrate: role of heat shock protein 70 and NF-κB. Am J Physiol Gastrointest Liver Physiol 2003;285:G177–84.
48. Boffa LC, Vidali G, Mann RS, Allfrey VG. Suppression of histone deacetylation in vivo and in vitro by sodium butyrate: reversible effects of Na-butyrate on histone acetylation. J Biol Chem 1978; 253:3364–6.
49. Vidali G, Boffa LC, Mann RS, Allfrey VG. Reversible effects of Na-butyrate on histone acetylation. Biochem Biophys Res Commun 1978;82:223–7.
50. Reeves R, Gorman CM, Howard B. Minichromosome assembly of non-integrated plasmid DNA transfected into mammalian cells. Nucleic Acids Res 1985;13:3599–615.

Available online at www.sciencedirect.com
SCIENCE DIRECT®
ELSEVIER
Immunology Letters 99 (2005) 193–197
Immunology Letters
www.elsevier.com/locate/

TCRαβ repertoire diversity of human naturally occurring CD4+CD25+ regulatory T cells

Masumi Fujishima, Makoto Hirokawa*, Naohito Fujishima, Ken-ichi Sawada

Division of Hematology and Oncology, Department of Medicine III, Akita University School of Medicine, 1-1-1 Hondo, Akita 0108543, Japan

Received 1 December 2004; received in revised form 20 February 2005; accepted 21 February 2005
Available online 23 March 2005

Abstract

We examined the αβ T cell receptor (TCR) repertoire of naturally occurring CD4+CD25+ regulatory T (Treg) cells isolated from healthy human blood. Three-color FACS analysis demonstrated that the usage of variable region segments of TCRβ chains by CD4+CD25+ cells did not differ from those of CD4+CD25− cells. Complementarity-determining region 3 (CDR3) size distribution analyses demonstrated that the repertoire diversity of CDR3β was almost identical between CD4+CD25+ and CD4+CD25− T cell subsets, and that there was no skewing of the CDR3β repertoire of CD4+CD25+ T cells. In contrast, in vitro activated CD4+CD25+ T cells by cytomegalovirus-derived antigens showed a skewed CDR3 size distribution pattern. These findings support the hypothesis that naturally occurring CD4+CD25+ T cell subset in humans is largely composed of a T cell lineage positively selected in the thymus as a consequence of the interaction between self-peptides and TCRs and not derived from recent activation by a limited array of antigens.

Keywords: CD4+CD25+ regulatory T cells; Human; TCR repertoire

Naturally occurring CD4+CD25+ T lymphocytes (nTreg) have been initially characterized by their role in maintaining peripheral tolerance in mice [1]. The forkhead transcription factor *Foxp3* gene has recently been shown to be a master gene for the generation of nTreg cells in the thymus [2]. The naturally occurring CD4+CD25+ regulatory T cells expressing *Foxp3* gene transcription were also identified in humans, and accumulating evidence has shown that conventional CD4+CD25− T cells can also upregulate expression of the *Foxp3* as well as CD25 and acquire immunosuppressive effects in vitro [3].

The normal T cell repertoire in mice and humans contains nTreg that control autoaggressive immune responses [1,3]. Jordan et al. reported that murine CD4+CD25+ regulatory T cells are positively selected in the thymus as a consequence of interaction between a self peptide and high-affinity TCRs [4]. If this is the case with humans as well as in mice, TCR repertoires of CD4+CD25+ T cells in human blood should be as diverse as those of CD4+CD25− T cells. Conversely, if the CD4+CD25+ T cell subset in circulating blood represents recently activated T cells, TCR repertoires should be skewed. In the present study, we compared αβTCR repertoires of human peripheral blood CD4+CD25+ T cells to those of CD4+CD25− T cells.

Peripheral blood mononuclear cells (PBMCs) were isolated from heparinized blood of healthy volunteer donors by the Ficoll–Conray gradient centrifugation method. The usage of TCRβ variable gene segments by the CD4+CD25+ and CD4+CD25− T cell subsets were determined by three-color flow cytometry using FACS Calibur (Becton Dickinson). Cy5-labeled CD4 and FITC-labeled CD25 were purchased from Becton Dickinson (Mountain View, CA). PE-labeled mAbs specific for TCRBV were obtained from Immunotech (Marseille, France). Purification of CD4+CD25+ cells were isolated from PBMCs using a human CD4+CD25+ regulatory T cell isolation kit (Miltenyi Biotec, Germany) combined with a Mini-MACS system according to the manufacturer's instruction. Diversity of the CDR3β region was determined by CDR3 size spectratyping analysis. Total RNA

* Corresponding author. Tel.: +81 18 884 6116; fax: +81 18 836 2613.
E-mail address: hirokawa@cna.ne.jp (M. Hirokawa).

0165-2478/$ – see front matter © 2005 Elsevier B.V. All rights reserved.
doi:10.1016/j.imlet.2005.02.011

was extracted from purified T cell subsets using an RNeasy Total RNA Kit (Qiagen, Hilden, Germany). Complementary DNA (cDNA) was synthesized using a First-Strand cDNA Synthesis Kit with an oligo-dT primer (Amersham Pharmacia Biotech, Uppsala, Sweden). Aliquots of cDNA were amplified using Vβ-specific and Cβ-specific primers. Sequences of the Vβ and Cβ primers were previously reported [5,6]. Sequences were amplified by PCR in a 20 μl reaction mixture containing 0.2 μM of each primer and 0.5 U of *Taq* polymerase (TaKaRa, Osaka, Japan) in 10 mM Tris–HCl (pH 8.3), 50 mM KCl, 1.5 mM $MgCl_2$, and 0.2 mM of each dNTP. The amplification conditions consisted of 40 cycles of denaturation at 94 °C for 1 min, annealing at 55 °C for 1 min, and extension at 72 °C for 1.5 min followed by a single extension at 72 °C for 15 min. Aliquots (4 μl) of unlabeled Vβ–Cβ PCR products were subjected to one cycle of elongation (runoff reaction) with a FAM-labeled nested Cβ primer (FAM-CB3) under the following conditions: denaturation at 94 °C for 2 min, annealing at 55 °C for 1 min, and extension at 72 °C for 15 min in the buffer described above. Labeled PCR products were mixed with a size marker (GeneScan-500 TAMRA, Applied Biosystems, Warrington, UK), and resolved on 5% polyacrylamide sequencing gels. Size and fluorescence intensity of the products were determined using an automated DNA sequencer (ABI 377, Perkin-Elmer Applied Biosystems, Foster, CA, USA). Data were analyzed using GeneScan software (Perkin-Elmer Applied Biosystems). The CD4+CD25+ or CD4+CD25− T cells were incubated with irradiated allogeneic or autologous dendritic cells. Responder T lymphocytes were prepared as previously described. Monocyte-derived dendritic cells (DCs) were prepared from plastic adherent cells followed by cultivation in the presence of GM-CSF and IL-4. Stimulator dendritic cells were irradiated (3000 rad), then were co-cultured with responder T cells (1×10^5 cells/well) in RPMI1640 containing 10% heat-inactivated autologous serum in round-bottom 96-well microtiter plates. [^{3}H] thymidine (1 μCi/well) was added to each well on day 4. After 18 h, cells were harvested, and radioactivity was measured by a liquid scintillation counter (TopCount NXT; Perkin-Elmer LAS, Boston, USA). For detection and quantification of mRNA levels of *Foxp3*, LightCycler technology (Roche Molecular Biochemicals, Mannheim, Germany) was used according to the manufacturer's instructions. For relative quantification, beta-actin mRNA served as an external control. PCR reactions were performed using a QuantiTect™ SYBR Green PCR Kit (Qiagen, Hilden, Germany). PCR was carried out in a final volume of 20 μL using each primer at 0.5, 4 μM $MgCl_2$, 2 μL of supplied enzyme mix containing the reaction buffer, FastStart *Taq* DNA polymerase, and DNA double-strand-specific SYBR Green I dye for detection of PCR products. PCR was performed in a LightCycler with a 900 s preincubation at 95 °C followed by 40 cycles of 15 s at 95 °C, 20 s at 59 °C, and 20 s at 72 °C. The following primers were used: beta actin-specific forward primer 5′-CAAGAGATGGCCACGGCTGCT-3′, reverse primer 5′-TCCTTCTGCATCCTGTCGGCA-3′; *Foxp3*-specific forward primer 5′-GCAAATGGTGTCTGCAAGTGG-3′, reverse primer 5′-CACTCAGCTTCTCCTTCTCCA-3′. Analyses of the quantitative real-time PCR curves were performed using the LightCycler 3.5 software. The beta actin control reflected the amount of target mRNA in each sample. Two independent samples of T cell subsets were examined in duplicate.

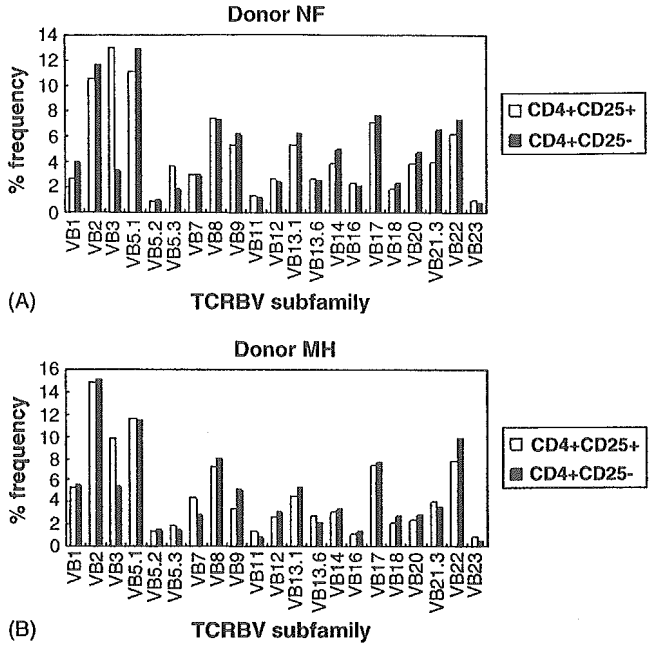

Fig. 1. TCRBV repertoires of CD4+CD25+ and CD4+CD25− T cells in two healthy individuals were analyzed by three-color FACS analysis using a panel of 21 Vβ-specific mAbs.

We firstly examined variable region repertoires of TCRβ chains (TCRBV repertoires) used by CD4+CD25+ and CD4+CD25− T cell subsets in two healthy individuals by three-color FACS analysis. TCRBV repertoires of the CD4+CD25+ T cell subset were quite similar to those of the CD4+CD25− T cell subset except for the preferential usage of Vβ3 by the CD4+CD25+ T cells (Fig. 1). Next, we investigated whether clonal restriction would be observed in nTreg cells by CDR3β size distribution analysis. CD4+CD25+ T cells were isolated from PBMCs by magnetic cell sorting as described above. Purity of the separated CD4+CD25+ T cell subset was 82.9%. Proliferative response of the CD4+CD25+ T cells against allogeneic stimulation with irradiated DCs was much lower than that of CD4+CD25− T cells, and expression of *Foxp3* gene by the purified CD4+CD25+ T cells was much higher than that of CD4+CD25− T cells (Fig. 2); both findings are consistent with those previously reported (3). Neither CD4+CD25+ nor CD4+CD25− T cells responded against irradiated autologous DCs. Using these purified T cells, the CDR3β diversity was examined by spectratyping analysis. As shown in Fig. 3, CDR3β size distribution patterns of CD4+CD25+ T cells were highly diverse and showed almost similar patterns to those of the CD4+CD25− T cells (Fig. 3). In contrast, CD4+CD25+ T cells purified from in

vitro activated PBMCs by CMV-derived antigens showed a skewed CDR3 size distribution pattern (Fig. 3).

These results demonstrate that the repertoire of human nTreg cells is as highly diverse as that of the CD4+CD25− T cells, implying that the CD4+CD25+ T cell subset is not merely a recently activated T cell population that recognizes a limited set of antigens in humans as in mice. Jordan et al. and other groups have demonstrated that self-reactive T cells are

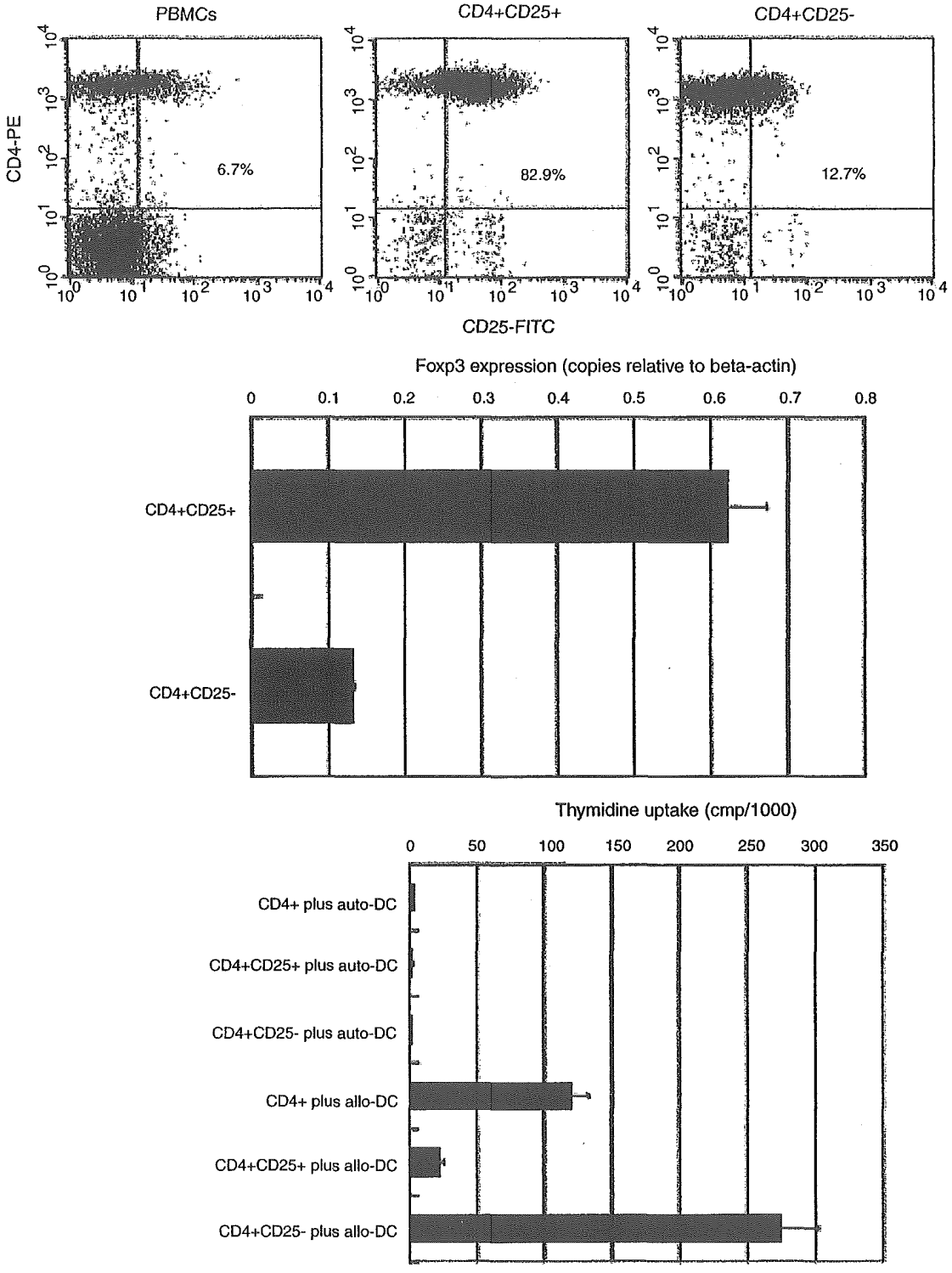

Fig. 2. *Foxp3* expression and proliferative response of freshly isolated regulatory CD4+CD25+ T cells against allogeneic stimulation. Unfractionated or fractionated CD4+ T cells were cultured with irradiated autologous or allogeneic DCs. The thymidine uptake data are presented as the mean ± S.D. of triplicate cultures. These experiments were repeated once with the similar results.

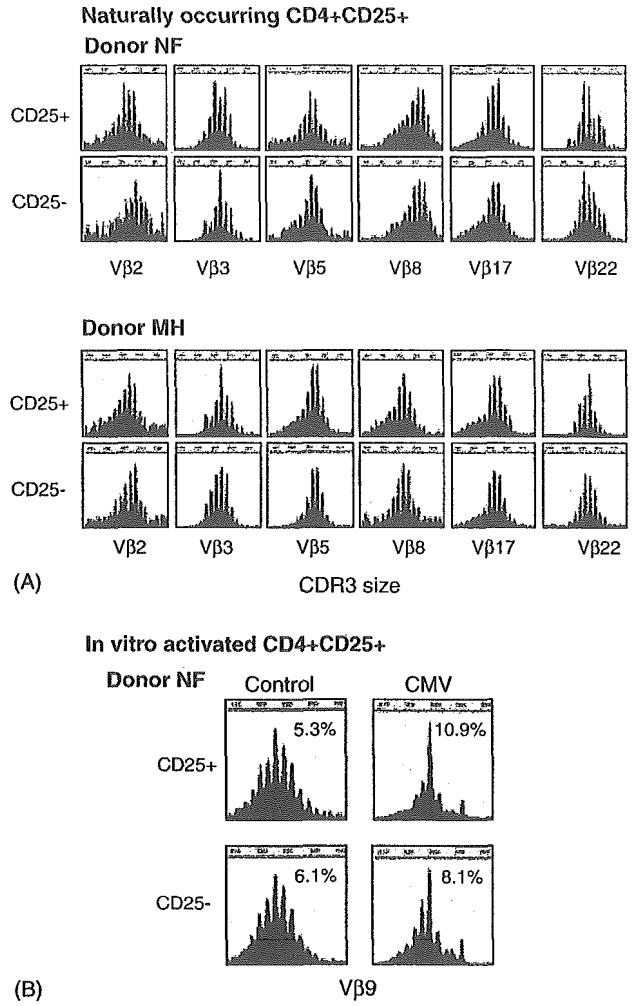

Fig. 3. Comparison of CDR3β size distribution patterns between naturally occurring regulatory CD4+CD25+ T cells and CD4+CD25− T cells from healthy individuals (A). In a separate experiment, PBMCs were stimulated with the extract of cytomegalovirus AD-169-infected cells (Chemicon, Temecula, CA) for 7 days. TCRVβ repertoires of in vitro stimulated CD4+CD25+ and CD4+CD25− T cells were analyzed by flow cytometry, and the increased usage of TCRVβ9 by the CD4+CD25+ subset was identified. The CD4+CD25+ and CD4+CD25− T cells were purified, and then CDR3 size distribution patterns of TCRVβ9 were analyzed (B).

positively selected as CD4+CD25+ regulatory T cells and are not deleted in the thymus [7,8]. Since self-peptides presented in the thymus should include a wide array of autoantigens, it is reasonable to interpret our data as reflecting the positive selection of CD4+CD25+ regulatory T cells in the thymus which can recognize self-peptides. Battaglia et al. have recently demonstrated that there is a correlation of the TCRVβ expression in peripheral blood between the CD4+CD25− and the CD4+CD25+ T cell subsets [9], which is consistent with our results. They have also shown that the TCRVβ repertoire is different between CD4+CD25+ regulatory T cells from peripheral blood and those from lymph nodes. Although they do not demonstrate the clonality data, these results suggest that the antigenic milieu of lymph nodes may exert a selective pressure on shaping the TCR repertoire of CD4+CD25+ regulatory T lymphocytes. With regard to the preferential usage of TCRVβ3 by CD25+ T cells in the present study, it is not yet clear whether this difference is consistent or biologically significant, since only a limited number of donors have been examined. CDR3 size spectratyping analysis demonstrated no skewing in both donors in the present study, suggesting that at least this TCRVβ subfamily was not used by recently activated CD4+ T cells. Antigen-induced regulatory T cells can be obtained by various means of providing regulatory signals to T cells in vitro, and these antigen-induced regulatory T cells express either CD8+ or CD4+ depending upon experimental protocols [10]. Thus, we are not able to exclude the possibility that the CD4+CD25+ T cell subset in human peripheral blood includes antigen-induced regulatory T cells. However, polyclonality of the CD4+CD25+ T cell population appears to suggest that the majority of this subset may be naturally occurring regulatory cells but not antigen-induced regulatory cells.

Acknowledgment

Supported by a grant from the Ministry of Education, Science, Sports and Culture of Japan (14570960) to MH.

References

[1] Sakaguchi S, Sakaguchi N, Asano M, Itoh M, Toda M. Immunologic self-tolerance maintained by activated T cells expressing IL-2 receptor alpha-chains (CD25). Breakdown of a single mechanism of self-tolerance causes various autoimmune diseases. J Immunol 1995;155:1151–64.

[2] Hori S, Nomura T, Sakaguchi S. Control of regulatory T cell development by the transcription factor Foxp3. Science 2003;299:1057–61.

[3] Walker MR, Kasprowicz DJ, Gersuk VH, Benard A, Van Landeghen M, Buckner JH, et al. Induction of FoxP3 and acquisition of T regulatory activity by stimulated human CD4+CD25− T cells. J Clin Invest 2003;112:1437–43.

[4] Jordan MS, Boesteanu A, Reed AJ, Petrone AL, Holenbeck AE, Lerman MA, et al. Thymic selection of CD4+CD25+ regulatory T cells induced by an agonist self-peptide. Nat Immunol 2001;2:301–6.

[5] Hirokawa M, Horiuchi T, Kitabayashi A, Kawabata Y, Matsutani T, Suzuki R, et al. Delayed recovery of CDR3 complexity of the T cell receptor β chain in recipients of allogeneic bone marrow transplants who had virus-associated interstitial pneumonia: monitor of T-cell function by CDR3 spectratyping. J Allergy Clin Immunol 2000;106:32–9.

[6] Saitoh H, Hirokawa M, Fujishima N, Ichikawa Y, Kawabata Y, Miura I, et al. The presence and longevity of peripherally expanded donor-derived TCRαβ+ mature T lymphocyte clones after allogeneic bone marrow transplantation for adult myeloid leukemias. Leukemia 2003;17:1626–35.

[7] Romagnoli P, Hudrisier D, van Meerwijk JPM. Preferential recognition of self antigens despite normal thymic deletion of CD4+CD25+ regulatory T cells. J Immunol 2002;168:1644–8.

[8] Kawahata K, Misaki Y, Yamauchi M, Tsunekawa S, Setoguchi K, Miyazaki J, et al. Generation of CD4+CD25+ regulatory T cells from

autoreactive T cells simultaneously with their negative selection in the thymus and from nonautoreactive T cells by endogenous TCR expression. J Immunol 2002;168:4399–405.
[9] Battaglia A, Ferrandina G, Buzzonetti A, Malinconico P, Legge F, Salutari V, et al. Lymphocyte populations in human lymph nodes. Alterations in CD4+CD25+ T regulatory cell phenotype and T-cell receptor Vβ repertoire. Immunology 2003;110:304–12.
[10] Vigouroux S, Yvon E, Brenner MK. Antigen-induced regulatory T cells. Blood 2004;104:26–33.

Nephrol Dial Transplant (2005) 20: 539–544
doi:10.1093/ndt/gfh673

Nephrology
Dialysis
Transplantation

Original Article

Up-regulation of *TRAIL* mRNA expression in peripheral blood mononuclear cells from patients with minimal-change nephrotic syndrome

Shin Okuyama, Atsushi Komatsuda, Hideki Wakui, Namiko Aiba, Naohito Fujishima, Keiko Iwamoto, Hiroshi Ohtani and Ken-ichi Sawada

Third Department of Internal Medicine, Akita University School of Medicine, Akita, Japan

Abstract

Background. Minimal-change nephrotic syndrome (MCNS) is considered to be associated with T-cell dysfunction and with the abnormal secretion of putative glomerular permeability factors; however, the nature of such factors remains elusive.

Methods. To identify up-regulated genes during the nephrosis phase, we undertook serial analyses of gene expression (SAGE) in peripheral blood mononuclear cells (PBMC) from a patient with MCNS sampled during the nephrosis and remission phases. To confirm the SAGE results, we performed quantitative real-time reverse transcription–polymerase chain reaction (RT–PCR) analyses. We also measured the serum levels of the identified gene product in nephrosis and remission samples from 29 MCNS patients, 57 patients with nephrotic syndrome due to other types of glomerular diseases and 30 healthy individuals.

Results. Using more than 20 000 SAGE tags, we identified 15 functionally known genes that were up-regulated (≥4-fold) in PBMC from the MCNS patient during the nephrosis phase. For further examination, we selected two genes encoding secretory proteins, namely tumour necrosis factor-related apoptosis-inducing ligand (TRAIL) and tissue inhibitor of metalloprotease 1. Real-time RT–PCR analysis confirmed a higher expression of *TRAIL* mRNA in PBMC during nephrosis than during remission in eight MCNS patients. The expression pattern of *TRAIL* mRNA, however, was variable among four patients with membranous nephropathy. There was no significant increase of serum levels of a soluble form of TRAIL in MCNS patients during the nephrosis phase.

Conclusions. These results suggest that the intracellular *TRAIL* mRNA expression in PBMC is up-regulated in MCNS patients during the nephrosis phase. This change may represent either an epiphenomenon or it may provide a potential explanation for the altered T-cell function in MCNS.

Keywords: gene expression profile; minimal-change nephrotic syndrome; serial analysis of gene expression; tumour necrosis factor-related apoptosis-inducing ligand

Introduction

Minimal-change nephrotic syndrome (MCNS) is a clinicopathological entity defined by selective massive proteinuria, and a relapsing and remitting course, without histological evidence of classic immune-mechanism mediated injury [1]. MCNS is considered to be associated with T-cell dysfunction. Abnormal soluble factors produced by activated T-cells might alter the permeability of the glomerular filtration barrier [1]. In fact, experimental studies have shown that peripheral blood mononuclear cells (PBMC) and T-cell hybridomas derived from patients with MCNS could produce proteinuria-inducing factors in rats [2,3]. Pegoraro *et al.* [4] also demonstrated that serum from patients with MCNS altered the albumin permeability of monolayers of cultured rat glomerular epithelial cells. Circulating humoral factors are, therefore, likely to have important roles in the pathogenesis of MCNS. Although the nature of these factors remains elusive, several studies have suggested that cytokines, such as interleukin-2 and interferon (IFN)-γ, are involved in the development of MCNS [5 and references therein].

Recently, Sahali *et al.* [6], screening a library of subtracted cDNA, reported on a novel approach for

Correspondence and offprint requests to: Atsushi Komatsuda, MD, Third Department of Internal Medicine, Akita University School of Medicine, 1-1-1 Hondo, Akita City, Akita 010-8543, Japan.
Email: komatsud@med.akita-u.ac.jp

the identification of PBMC genes that are potentially involved MCNS relapse. Their preliminary screening of the library, with relapse and remission unsubtracted cDNA probes, identified approximately 1000 clones. They finally found 42 up-regulated known transcripts in MCNS relapse. These transcripts included genes encoding proteins associated with signalling pathways and the cytoskeletal scaffold.

Serial analysis of gene expression (SAGE), a recently developed functional genomic approach, has enabled us to identify simultaneously the expression pattern of thousands of genes [7]. Therefore, SAGE can be applied for comparing differences of gene expression between PBMC from MCNS patients during the nephrosis and remission phases. In the present study, we capitalized on an advantage of SAGE for screening of mRNA expression in PBMC from a MCNS patient during the two phases. Among the up-regulated genes in the nephrosis sample, two were for secretory proteins, namely tumour necrosis factor (TNF)-related apoptosis-inducing ligand (TRAIL) (approved gene symbol *TNFSF10*) [8,9] and tissue inhibitor of metalloprotease 1 (TIMP-1). We selected these genes for further examinations.

Subjects and methods

Patients

The one patient selected for construction of a SAGE library was a 42-year-old Japanese woman, Patient 1, who visited us with acute onset of nephrotic syndrome on 6 December 2001. On physical examination, she had oedema in the legs and a blood pressure of 168/98 mmHg. Her urinalysis was 3+ positive for protein without haematuria. Her total 24-h urinary protein was 12.5 g, serum total protein 4.9 g/dl, albumin 2.2 g/dl, blood urea nitrogen 7.1 mg/dl, creatinine 0.6 mg/dl, creatinine clearance 106.8 ml/min, leukocyte count 11 200/μl, haemoglobin 13.2 g/dl and platelet count 34.1×10^4/μl. Her serum immunoglobulins were normal and her anti-nuclear antibodies, anti-neutrophil cytoplasmic antibodies and cryoglobulins were negative. Serum complement C3 was 193 mg/dl, C4 23.5 mg/dl and CH50 42.5 U/ml. Circulating immune complexes were not detected by the C1q-binding assay. Serum and urine electrophoresis showed no monoclonal proteins. A renal biopsy revealed minimal changes in 16 glomeruli, without mesangial proliferation, interstitial cell infiltration or focal segmental glomerulosclerosis (FSGS). Immunofluorescence stainings for immunoglobulin (Ig)-G, IgA, IgM, κ, λ, C3, C1q and fibrinogen yielded negative results.

Based on these findings, she was diagnosed to have MCNS and was treated with prednisolone (40 mg/day). With the treatment, she reached complete remission within 2 weeks. While her dosage of prednisolone was being tapered, her MCNS relapsed. Blood samples were obtained from her during the relapse in August 2002 (while the patient was receiving 15 mg/day prednisolone) and 3 months after the remission of this episode of relapse (while the patient was receiving 15 mg/day prednisolone therapy).

In this study, we also examined blood samples from 29 patients during the nephrosis and remission phases with biopsy-proven MCNS, 30 healthy subjects and 57 patients with nephrotic syndrome [biopsy-proven; 27 with FSGS and 30 with membranous nephropathy (MN)]. The protocol of this study was approved by the ethics committee of the institution involved and informed consent for genetic studies was obtained from all subjects.

SAGE protocol

The libraries for SAGE of PBMC from Patient 1 during nephrosis and remission phases were generated as described previously [10]. Total RNA was prepared using a Trizol reagent (Gibco-BRL, Gaithersburg, MD, USA). PolyA+ RNA was obtained using a Messagemaker kit (Gibco-BRL) according to the manufacturer's instruction and was converted to cDNA with a SuperScript Choice System (Gibco-BRL) with a 5′-biotinylated oligo(dT). Biotinylated double-strand cDNA was cleaved with the restriction enzyme *Nla*III (New England Biolaboratories, Beverly, MA, USA) and the 3′-terminal fragments were bound to streptoavidin-coated magnetic beads (Dynal, Oslo, Norway). Captured 3′ cDNA fragments were divided into two pools and each pool was ligated to one of the linkers containing recognition sites for *Bsm*FI.

Nucleotide sequences of the linkers were as follows:

Linker 1 5′-TTTGGATTTGCTGGTGCAGTACAACT
AGGCTTAATAGGGACATG-3′
5′-TCCCTATTAAGCCTAGTTGTACTGCA
CCAGCAAATCC[amino modifier C5]-3′

Linker 2 5′-TTTCTGCTCGAATTCAAGCTTCTAAC
GATGTACGGGGACATG-3′
5′-TCCCCGTACATCGTTAGAAGCTTGAA
TTCGAGCAG[amino modifier C5]-3′

Linkered cDNAs were released from the beads by digestion with *Bsm*FI. After digestion, the linker tags were blunted with Klenow fragments and were ligated to each other to generate 'ditags' (tags ligated tail-to-tail). The ditags were amplified with polymerase chain reaction (PCR) in 32 cycles, with 5′-GGATTTGCTGGTGCAGTACA-3′ and 5′-CTGCT CGAATTCAAGCTTCT-3′ as primers.

PCR products were analysed by polyacrylamide gel electrophoresis (PAGE) and the band containing the ditags was excised. After digestion with *Nla*III, the ditags were ligated together to produce concatemers. The concatemers were separated by PAGE, and the products that consisted of between 400 and 1200 base pairs (bp) were excised. These products were cloned into pZero-1 (Invitrogen, Carlsbad, CA, USA), digested with *Sph*I (New England Biolaboratories). PCR for insert screening of colonies was performed with the M13 forward and reverse sequences as primers. PCR products longer than 600 bp were sequenced using the BigDye terminator cycle sequence kit (Perkin-Elmer Applied Biosystems, Foster City, CA, USA). Sequencing was performed with an ABI 377 automated DNA sequencer (Perkin-Elmer Applied Biosystems).

SAGE data analysis

Concatemer sequences were analysed as described previously [10] with the SAGE 2000 software, version 4.12, which was kindly provided by Dr Kinzler (Johns Hopkins University). To identify the individual genes, the search for the expressed

genes was conducted at the Serial Analysis of Gene Expression Tag of the Gene Mapping home page (http://www.ncbi.nlm.gov/SAGE). The detailed SAGE protocol can be seen at the SAGE home page (http://www.sagenet.org).

Quantitative real-time RT–PCR

We quantified *TRAIL* and *TIMP-1* mRNA expressions in the nephrosis and remission PBMC samples from four MCNS patients (including Patient 1) and eight MN patients. Table 1 summarizes the medical regimens of these patients at the time blood samples were obtained.

Total RNA was prepared with an RNeasy kit (Qiagen, Hilden, Germany) and used for cDNA synthesis with an oligo(dT) primer (Amersham Biosciences, Piscataway, NJ, USA), as described previously [10]. The following PCR primers were used:

TRAIL-specific forward primer	5′-ATGGCTATGATGG AGGTCCAG-3′
TRAIL-specific reverse primer	5′-TTGTCCTGCATCT GCTTCAGC-3′
TIMP-1-specific forward primer	5′-CTGTTGTTGCTG TGGCTGATA-3′
TIMP-1-specific reverse primer	5′-CCGTCCACAAGCA ATGAGT-3′
β-actin-specific forward primer	5′-CAAGAGATGGCC ACGGCTGCT-3′
β-actin-specific reverse primer	5′-TCCTTCTGCATCC TGTCGGCA-3′

We confirmed that each PCR product had a single band on agarose gel electrophoresis and that each of the sequence data were correct.

Real-time reverse transcription (RT)–PCR reaction was carried out according to the manufacturer's instructions in a final 20 µl volume containing 10 µl DNA Master Hybridization Probe 2X (Qiagen), 1 µl of 10 pmol forward and reverse primers, 1 µl cDNA and 7 µl water. After an initial denaturation step at 95°C for 900 s, temperature cycling was initiated. Each cycle consisted of denaturation at 95°C for 15 s, hybridization at 56°C (for *TRAIL* and *β-actin*) or at 60°C (for *TIMP-1*) for 20 s and elongation at 72°C for 20 s, using a LightCycler (Roche Diagnostics, Mannheim, Germany). Forty-five cycles were performed and each sample was run in triplicate.

Quantitative real-time RT–PCR curves were analysed by the LightCycler 3.5 software (Roche Diagnostics). For the relative quantification of *TRAIL* and *TIMP-1* mRNA expressions, the mRNA expression of *β-actin* was used as a control.

ELISA for a soluble form of TRAIL

Serum levels of a soluble form of TRAIL (sTRAIL) were measured in duplicate for each sample, using an enzyme-linked immunosorbent assay (ELISA) kit for sTRAIL (Active Motif North America, Carlsbad, CA, USA). Optical density was measured in an ELISA reader at 405 nm. Concentrations of sTRAIL were determined by a standard curve, according to the manufacturer's instructions.

Results

Generation and analysis of SAGE tags from PBMC from an MCNS patient during nephrosis and remission phases

SAGE libraries were constructed from PBMC obtained from Patient 1 during nephrosis and

Table 1. Profiles and data of patients with MCNS and MN examined by real-time RT-PCR

Patient no.	Age	Sex	Onset or relapse[a]			Remission			Real-time RT–PCR[b]		sTRAIL (ng/ml)	
			PSL (mg)	AZP (mg)	CsA (mg)	PSL (mg)	AZP (mg)	CsA (mg)	*TRAIL*	*TIMP-1*	Onset or relapse	Remission
1	42	F	15	0	0	15	0	0	5.4	4.6	0.3	0.3
2	55	M	15	50	0	40	0	0	6.2	2.8	0.5	0.3
3	44	F	5	0	0	15	50	0	1.9	0.8	0.8	0.3
4	18	M	0	0	0	25	0	0	6.6	0.8	0.8	0.5
5	38	M	0	0	0	25	0	0	14.1	0.9	0.3	0.3
6	16	F	27.5	0	200	40	0	300	1.9	1.0	0.4	0.4
7	20	M	0	0	0	40	0	0	4.3	1.3	0.2	0.2
8	22	F	0	0	0	12.5	0	0	1.9	1.4	0.1	0.1
9	75	M	0	0	0	0	0	0	0.4	ND	0.1	0.1
10	51	M	0	0	0	0	0	0	1.3	ND	0.3	0.3
11	58	F	0	0	0	15	0	0	1.5	ND	0.1	0.1
12	70	F	0	0	0	15	0	0	0.6	ND	0.1	0.1

Patient numbers 1–8, patients with MCNS; patient numbers 9–12, patients with MN.
Samples from Patient 1 were used for SAGE.
[a]Blood samples were obtained from patients 4, 5 and 7–12 at the onset, before the beginning of therapy and from the remaining four patients with MCNS in relapse; the daily doses of the tapering dosage of PSL are indicated, with or without other immunosuppressive agents.
[b]Real-time RT–PCR was performed as described in the text. For relative quantification of *TRAIL* and *TIMP-1* mRNA expressions, the mRNA expression of *β-actin* was used as a control. The indicated values are the ratios of the means of the relative numbers of mRNA copies (onset or relapse/remission).
AZP, azathioprine; CsA, cyclosporin A; F, female; M, male; ND, not done; PSL, prednisolone.

remission phases. We obtained 10606 tags from a nephrosis sample and 10171 tags from a remission sample. Using these SAGE tags, we searched for up- and down-regulated genes in the nephrosis PBMC sample. Tables 2 and 3 list the tags differentially expressed in the nephrosis PBMC sample at levels >4-fold higher or lower, respectively, than in the remission sample. In Tables 2 and 3, we have listed GenBank matches of tags derived from functionally known genes, except for genes for ribosomal proteins.

Among up-regulated genes in the nephrosis PBMC sample (Table 2), there were genes for secretory proteins (TRAIL and TIMP-1) and genes for proteins involved in signalling pathways (calcium/calmodulin-dependent protein kinase kinase 1, mitogen-activated protein kinase-activated protein kinase 2, FK506 binding protein 1A and cyclophilin F). On the other hand, down-regulated genes in the nephrosis PMBC sample mainly encoded membrane-associated proteins (Table 3).

Quantification of TRAIL and TIMP-1 mRNA expressions in PBMC from MCNS patients during nephrosis and remission phases by real-time RT–PCR

SAGE showed that two genes for secretory proteins (TRAIL and TIMP-1) were up-regulated in the PBMC from Patient 1 during the nephrosis phase of MCNS (Table 2). To confirm this result, we performed quantitative real-time RT–PCR analyses for *TRAIL* and *TIMP-1* mRNA expressions in nephrosis and remission PBMC samples from seven additional MCNS patients. We confirmed that *TRAIL* mRNA expressions were higher in the nephrosis samples than in the remission samples from all the MCNS patients analysed (patients 1–8 in Table 1). On the other hand, we could not confirm that the expressions of *TIMP-1* mRNA in the nephrosis PBMC samples were higher than in the remission samples from all the MCNS patients (Table 1).

We also examined *TRAIL* mRNA expressions in the nephrosis and remission PBMC samples from

Table 2. Up-regulated PBMC gene transcripts from Patient 1 with MCNS in the nephrosis phase

	Tag	N	R	Symbol	Description
1	CCACTACACT	7	1	*TNFSF10*	TNF ligand superfamily, member 10[a]
2	GTGGTGGGTG	6	1	*SLC14A1*	Solute carrier family 14 A1
3	CATTTGTAAT	5	0	*CAMKK1*	Calcium/calmodulin-dependent protein kinase kinase 1, alpha
4	CGGCTGAATT	5	0	*PDG*	Phosphogluconate dehydrogenase
5	GAGAAATGGC	5	0	*MAPKAPK2*	Mitogen-activated protein kinase-activated protein kinase 2
6	GTAAAACCCT	5	0	*PECR*	Peroxisomal trans 2-enoyl CoA reductase
0	GAGAGTGTCT	4	0	*TIMP-1*	Tissue inhibitor of metalloprotease 1
8	TCTACTAATT	4	0	*EIF1A*	Eukaryotic translation initiation factor 1A
9	TGTGGGTGCT	4	0	*CDH1*	Cadherin 1, type 1, E-cadherin
10	GAGTAAAAAA	4	1	*PLA1A*	Phospholipase A1 member A
11	ACAAATCCTT	4	1	*FKBP1A*	FK506 binding protein 1A, 12 kDa
12	AGAATTGCTT	4	1	*PHKB*	Phosphorylase kinase, beta
13	CAAAATCAGG	4	1	*CCN1*	Cyclin 1
14	GATTTGTGTT	4	1	*PPIF*	Peptidylprolyl isomerase F, cyclophilin F
15	GGCTATGCCA	4	1	*LUC7A*	Cisplatin resistance-associated overexpressed protein

[a]TNF ligand superfamily, member 10 is also called TRAIL.
N, nephrosis phase; R, remission phase.

Table 3. Down-regulated PBMC gene transcripts from Patient 1 with MCNS in the nephrosis phase

	Tag	N	R	Symbol	Description
1	CCCAGCTAAT	1	6	*ALOX15*	Arachidonate 15-lipoxygenase
2	TCAGACGCAG	1	5	*PTMA*	Prothymosin, alpha
3	TTGTGATGTA	0	4	*TPM3*	Tropomyosin 3
4	GCGTGTGAGG	0	4	*KCNH2*	Potassium voltage-gated channel, subfamily H, member 2
5	CGCCGCGGTG	1	4	*EIF3S8*	Eukaryotic translation initiation factor 3, subunit 8, 110 kDa
6	GTTCAGCTGT	1	4	*VDAC2*	Voltage-dependent anion channel 2
7	CAGAGTGCTG	1	4	*VAPA*	Vesicle-associated membrane protein-associated protein A, 33 kDa
8	TGGCTGGGAA	1	4	*VAMP8*	Vesicle-associated membrane protein 8, endobrevin
9	TGAAACTCAT	1	4	*TPM3*	Tropomyosin 3
10	GCAAAACCCC	1	4	*TNFSF14*	TNF ligand superfamily, member 14
11	AGAGCTCACT	1	4	*SLC25A20*	Carnitine/acylcarnitine translocase, member 20

N, nephrosis phase; R, remission phasose.

four MN patients. The results showed that expression patterns were variable among these patients (patients 9–12 in Table 1).

Serum sTRAIL levels in MCNS patients during nephrosis and remission phases

Based on the results of SAGE and real-time RT–PCR analyses, we used ELISA to measure serum sTRAIL levels in 29 MCNS patients during the nephrosis and remission phases. We also measured serum sTRAIL levels in 30 healthy subjects and 57 patients with nephrotic syndrome due to other types of glomerular diseases (27 FSGS and 30 MN). The results showed that there was no significant increase in the serum sTRAIL level in MCNS patients during the nephrosis phase (Figure 1).

Discussion

In this study, we prepared for SAGE PBMC samples obtained from an MCNS patient during nephrosis and remission phases, and identified various up- and down-regulated genes in PBMC during the nephrosis phase. Since the MCNS samples were obtained while this patient received the same dosage of steroids during the two phases, the influence of steroids on the results of SAGE in this one patient can be excluded. For further studies, we selected two up-regulated genes encoding TRAIL and TIMP-1, which can be secreted by PBMC into the blood. Quantitative real-time RT–PCR analysis confirmed an increased *TRAIL* mRNA expression in nephrosis PBMC samples from all the MCNS patients examined. On the other hand, the *TRAIL* mRNA expression pattern was variable among nephrotic patients with MN. This suggests that the high *TRAIL* mRNA expression in the nephrosis PBMC samples from MCNS patients could not represent a condition associated with a nephrotic state. ELISA showed that there was no significant increase of serum sTRAIL levels in MCNS patients during the nephrosis phase.

Sahali *et al.* [6] recently reported their findings of a subtracted cDNA library screening, using cDNA from PBMC from the same MCNS patient and comparing the relapse and remission phases. They found various up-regulated PBMC transcripts for signalling pathways, including the mitogen-activated protein kinase cascade. Our SAGE results also showed considerable differences in the expression profiles between nephrosis and relapse PBMC samples from the same MCNS patient. During the nephrosis phase, there were several up-regulated genes for various proteins involved in signalling pathways, such as calcium/calmodulin-dependent protein kinase kinase 1, mitogen-activated protein kinase-activated protein kinase, FK506 binding protein 1A and cyclophilin F, in addition to the gene for *TRAIL*. These observations suggest that multiple signalling pathways might be activated in PBMC during the development of MCNS.

TRAIL (also known as Apo-2 ligand) has been identified as a member of the TNF ligand family that induces apoptosis in a wide variety of tumour cells [8,9]. TRAIL can selectively induce apoptosis in tumorigenic cells, but not in normal cells, highlighting its potential therapeutic application in cancer treatment. In contrast to other members of the TNF ligand family, which are often only transiently expressed on activated cells, *TRAIL* mRNA is expressed constitutively in a wide range of tissues [8]. Although TRAIL is primarily expressed as a type II transmembrane protein, bioactive sTRAIL might be released from activated T-cells in association with microvesicles or cleaved from the cell surface by proteases, or both [11,12]. Thus, the serum levels of sTRAIL are likely to be regulated not only by mRNA *TRAIL* expressions in PBMC but also by other factors. This might be the reason why in our study there was no correlation between the levels of mRNA *TRAIL* expression in PBMC and serum sTRAIL in MCNS patients during nephrosis.

Several studies have demonstrated that TRAIL is associated with the pathogenesis of some autoimmune diseases, such as neutropenia of systemic lupus erythematosus [13 and references therein]. However, there have been no reports suggesting the possibility

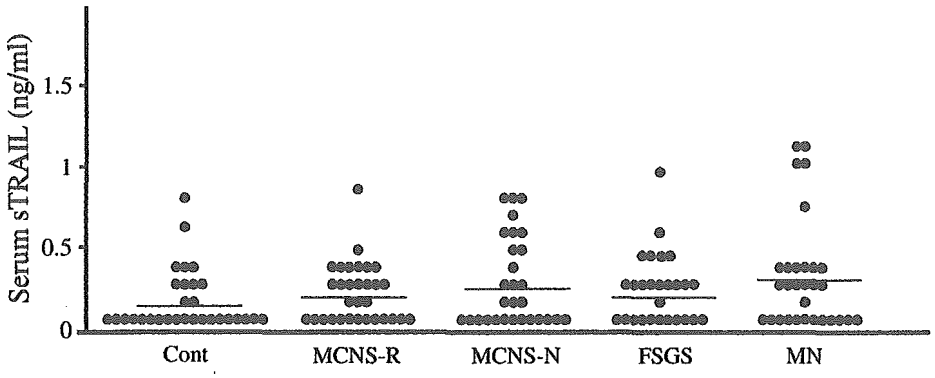

Fig. 1. ELISA for serum sTRAIL levels in patients with nephrotic syndrome and healthy individuals. We examined sera from 30 healthy individuals (Cont), 29 MCNS patients during both the nephrotic and remission phases (MCNS-N and MCNS-R), 27 patients with FSGS and 30 patients with MN. The bars indicate the median value for each group.

of TRAIL being associated with the pathogenesis of MCNS. Our results suggest that the intracellular *TRAIL* mRNA expression is up-regulated in PBMC during the nephrosis phase of MCNS, although the bulk of the investigations were based on preliminary SAGE findings from a single patient and real-time RT–PCR findings from a total of eight patients. Our observations could represent an epiphenomenon or they could provide a potential explanation for the altered T-cell function seen in MCNS.

It is known that therapeutic concentrations of IFN-β and IFN-α stimulate the expression of high levels of *TRAIL* mRNA in PBMC and neutrophils, and the release of elevated amounts of sTRAIL [14,15]. In fact, there are several case reports that describe an acute onset or a relapse of MCNS during the therapy of malignancies, or chronic viral hepatitis with IFN-β or IFN-α [16–19]. It is therefore possible that the up-regulation of a *TRAIL* induced by IFN-β or IFN-α might be involved in the development of MCNS in these cases. In particular, nephrotic-range proteinuria regressed without steroid treatment after the cessation of IFN-β injections in the case reported by Nakao *et al.* [17]. Although TRAIL is now considered to have a promising therapeutic potential in cancer treatment [20], careful patient monitoring, including urinalysis, will be necessary when using it.

Acknowledgements. This work was supported, in part, by the 21st Century COE Program from the Ministry of Education, Culture, Sports, Science and Technology of Japan.

Conflict of interest statement. None declared.

References

1. Falk RJ, Jennette JC, Nachman PH. Primary glomerular diseases: minimal change glomerulopathy. In: Brenner BM, ed. *The Kidney*, 7th edn. WB Saunders, Philadelphia, PA: 1301–1307
2. Yoshizawa N, Kusumi Y, Matsumoto K *et al.* Studies of a glomerular permeability factor in patients with minimal-change nephritic syndrome. *Nephron* 1989; 51: 370–376
3. Koyama A, Fujisaki M, Kobayashi M, Igarashi M, Narita M. A glomerular permeability factor produced by human T cell hybridomas. *Kidney Int* 1991; 40: 453–460
4. Pegoraro AA, Singh AK, Arruda JAL, Dunea G, Bakir AA. A simple method to detect an albumin permeability factor in the idiopathic nephrotic syndrome. *Kidney Int* 2000; 58: 1342–1345
5. Lama G, Luongo I, Tirino G *et al.* T-lymphocyte populations and cytokines in childhood nephrotic syndrome. *Am J Kidney Dis* 2002; 39: 958–965
6. Sahali D, Pawlak A, Valanciuté A *et al.* A novel approach to investigation of the pathogenesis of active minimal-change nephritic syndrome using subtracted cDNA library screening. *J Am Soc Nephrol* 2002; 13: 1238–1247
7. Ye SQ, Usher DC, Zhang LQ. Gene expression profiling of human diseases by serial analysis of gene expression. *J Biomed Sci* 2002; 9: 384–394
8. Wiley SR, Schooley K, Smolak PJ *et al.* Identification and characterization of a new member of the TNF family that induces apoptosis. *Immunity* 1995; 3: 673–682
9. MacFarlane M. TRAIL-induced signalling and apoptosis. *Toxicol Lett* 2003; 139: 89–97
10. Ichikawa Y, Hirokawa M, Aiba N *et al.* Monitoring the expression profiles of doxorubicin-resistant K562 human leukemia cells by serial analysis of gene expression. *Int J Hematol* 2004; 79: 276–282
11. Monlen I, Martinez-Lorenzo MJ, Monteagudo L *et al.* Differential secretion of Fas ligand- or APO2 ligand/TNF-related apoptosis-inducing ligand-carrying microvesicles during activation-induced death of human T cells. *J Immunol* 2001; 167: 6736–6744
12. Mariani SM, Krammer PH. Differential regulation of TRAIL and CD95 ligand in transformed cells of the T and B lymphocyte lineage. *Eur J Immunol* 1998; 28: 973–982
13. Matsuyama W, Yamamoto M, Higashimoto I *et al.* TNF-related apoptosis-inducing ligand is involved in neutropenia of systemic lupus erythematosus. *Blood* 2004; 104: 184–191
14. Wandinger K-P, Lunemann JD, Wengert O *et al.* TNF-related apoptosis inducing ligand (TRAIL) as a potential response marker for interferon-beta treatment in multiple sclerosis. *Lancet* 2003; 361: 2036–2043
15. Tecchio C, Huber V, Scapini P *et al.* IFNα-stimulated neutrophils and monocytes release a soluble form of TNF-related apoptosis-inducing ligand (TRAIL/Apo-2 ligand) displaying apoptotic activity on leukemic cells. *Blood* 2004; 103: 3837–3844
16. Traynor A, Kuzel T, Samuelson E, Wanwar Y. Minimal-change glomerulopathy and glomerular visceral epithelial hyperplasia associated with alpha-interferon therapy for cutaneous T-cell lymphoma. *Nephron* 1994; 67: 94–100
17. Nakao K, Sugiyama H, Makino E *et al.* Minimal-change nephrotic syndrome developing during postoperative interferon-beta therapy for malignant melanoma. *Nephron* 2002; 90: 498–500
18. Nishimura S, Miura H, Yamada H *et al.* Acute onset of nephrotic syndrome during interferon-α retreatment for chronic active hepatitis C. *J Gastroenterol* 2002; 37: 854–858
19. Dizer U, Beker CM, Yavuz I *et al.* Minimal change disease in patient receiving INF-alpha therapy for chronic hepatitis C virus infection. *J Interferon Cytokine Res* 2003; 23: 51–54
20. Kelley SK, Ashkenazi A. Targeting death receptors in cancer with Apo2L/TRAIL. *Curr Opin Pharmacol* 2004; 4: 333–339

Received for publication: 28.7.04
Accepted in revised form: 19.11.04

CASE REPORT

Development of Lupus Nephritis in a Patient With Human T-Cell Lymphotropic Virus Type I–Associated Myelopathy

Hideki Wakui, MD, Rie Masai, MD, Shin Okuyama, MD, Hiroshi Ohtani, MD, Atsushi Komatsuda, MD, Itaru Toyoshima, MD, Sumio Watanabe, MD, and Ken-ichi Sawada, MD

• **A 77-year-old Japanese man with a 14-year history of human T-cell lymphotropic virus type I–associated myelopathy developed pancytopenia, proteinuria, renal dysfunction, and hypocomplementemia. Antinuclear antibody and anti–double-stranded DNA antibody test results were positive, and circulating immune complexes were detected. A renal biopsy showed diffuse and global mesangiocapillary proliferation with extensive subendothelial deposits. Immunofluorescence microscopy showed strong granular staining for immunoglobulins and complements in the mesangium and along capillary walls. Electron microscopy showed numerous mesangial and subendothelial electron-dense deposits. From these findings, systemic lupus erythematosus and diffuse global lupus nephritis were diagnosed. This is a rare case of a patient developing lupus nephritis during the long-term course of human T-cell lymphotropic virus type I–associated myelopathy.** *Am J Kidney Dis* **46:E25-E29.**

INDEX WORDS: Human T-cell lymphotropic virus type I (HTLV-I); HTLV-I–associated myelopathy; systemic lupus erythematosus (SLE); lupus nephritis.

HUMAN T-CELL lymphotropic virus type I (HTLV-I), a member of a group of mammalian retroviruses, was discovered as the causative agent for adult T-cell leukemia (ATL).[1] Subsequently, HTLV-I was found to be associated with another human neurological disease, HLTV-I–associated myelopathy (HAM).[2] Approximately 5% to 10% of HTLV-I–infected individuals develop either ATL or HAM. Although a number of host and viral factors, including virus strain, viral load, and HLA haplotype, have been hypothesized to influence disease outcome associated with HTLV-I infection, the relative contributions of such factors to disease pathogenesis have not been fully established.[3]

HAM is a chronic progressive demyelinating disease that predominantly affects the spinal cord. Main neurological findings of HAM include gait disturbance caused by spastic paraparesis, urinary disturbance, sensory disturbance, and hyperreflexia with clonus and Babinski signs.[2] The occurrence of various autoimmune disorders, such as Sjögren syndrome, Behçet disease, and arthropathy, in patients with HAM also has been reported.[2]

Although the cause of systemic lupus erythematosus (SLE) remains unclear, human endogenous retroviruses recently were implicated as causative agents in patients with SLE.[4,5] The possibility that human exogenous retroviruses (HTLV-I and human immunodeficiency virus) may have an etiologic role in the development of SLE also has been discussed. Postulated roles for retroviruses in SLE include as intrinsic or mimicry antigens and/or stimulants of autoimmunity.[4,5] Although such roles of retroviruses have been defined in some murine lupus models, the pathogenetic role of HTLV-I in human SLE is still controversial.

Although 5 patients with SLE with ATL or HAM have been described in the literature,[6-9] there is only 1 case report on renal manifestations in a patient with ATL.[7] We report a patient with HAM who developed lupus nephritis during long-term follow-up and discuss a possible etiologic role for HTLV-I in patients with SLE.

CASE REPORT

A 77-year-old Japanese man was referred to Akita University Hospital (Akita City, Japan) for evaluation of proteinuria on December 3, 2004.

He had never received a blood transfusion. His mother was born in an HTLV-I–endemic area. His younger brother

From the Third and First Departments of Internal Medicine, Akita University School of Medicine, Akita City, Akita, Japan.

Received March 7, 2005; accepted in revised form May 9, 2005.

Originally published online as doi:10.1053/j.ajkd.2005.05.007 on June 21, 2005.

Address reprint requests to Hideki Wakui, MD, Third Department of Internal Medicine, Akita University School of Medicine, 1-1-1 Hondo, Akita City, Akita 010-8543, Japan. E-mail: wakui@med.akita-u.ac.jp

0272-6386/05/4602-0030$30.00/0

doi:10.1053/j.ajkd.2005.05.007

developed HAM at the age of 54 years in 1988. In July 2004, routine urinalysis and blood chemistry showed no findings suggesting the development of SLE in the brother. There was no family history of autoimmune disease.

The patient had been well until August 1990, when he developed gait and urinary disturbances. He was admitted to Akita University Hospital in November 1991 because these symptoms were slowly progressive. Neurological examination showed spastic gait, hyperreflexia of the lower limbs with ankle clonus and Babinski signs, and impaired vibration sense of the lower limbs. On urological examination, neurogenic bladder was noted. At that time, urine was negative for protein and occult blood. Hemoglobin level was 16.0 g/dL (160 g/L); white blood cell count, 5.1 × $10^3/\mu L$ (5.1 × 10^9/L) with 37% lymphocytes; and platelet count, 145 × $10^3/\mu L$ (145 × 10^9/L). Serum total-protein level was 7.0 g/dL (70 g/L); albumin, 4.4 g/dL (44 g/L); blood urea nitrogen, 23 mg/dL (8.2 mmol/L); and creatinine, 0.7 mg/dL (62 μmol/L). Antinuclear antibody test results were negative. CH50 level was 36.5 U/mL (normal range [NR], 30 to 50 U/mL). Lumbar puncture showed normal cerebrospinal fluid pressure. Analysis of cerebrospinal fluid showed 4 mononuclear cells/μL; protein, 15 mg/dL; and glucose, 72 mg/dL (4.0 mmol/L). Magnetic resonance imaging showed atrophy of the thoracic spinal cord. Anti–HTLV-I antibodies were detected by means of the particle agglutination method. Antibody titers in serum and cerebrospinal fluid were 1,024-fold and 2-fold, respectively.

From these findings, HAM was diagnosed, and he was treated with steroids. From February 1992, he was treated in the outpatient clinic. Treatment was partially effective for gait disturbance, but neurological symptoms were slowly progressive.

The patient had discontinued steroid therapy in a tapering course by himself in 1995. From 1997, he needed support in walking. On May 21, 2003, he was admitted to Akita University Hospital because of dysarthria caused by ischemia in the left posterior limb of the internal capsule. He was unable to walk. Sigmoid colon cancer was found, and a sigmoidectomy was performed August 4. From September 2003, he was followed up in a local hospital. Clean intermittent urethral catheterization was needed for his bladder dysfunction. In February 2004, he developed pancytopenia: hemoglobin level was 10.2 g/dL (102 g/L); white blood cell count, 2.2 × $10^3/\mu L$ (2.2 × 10^9/L); and platelet count, 65 × $10^3/\mu L$ (65 × 10^9/L). Bone marrow aspiration showed no evidence of malignancy. In April 2004, computed tomographic scans of the chest and abdomen showed no findings of colon cancer recurrence or metastasis, but pericardial effusion, pleural effusion, and ascites were observed. In November 2004, massive proteinuria (protein, 546 mg/dL) and hypoproteinemia were found.

On admission, physical examination showed pale conjunctiva, ascites, pitting pedal edema, and paralytic contracture of the lower limbs.

Total urinary protein level for 24 hours was 2.7 g, and urine sediments showed 5 to 9 red blood cells and greater than 100 white blood cells/high-power field. Urine cultures were positive for *Pseudomonas aeruginosa* and *Proteus mirabilis*. Hemoglobin level was 7.9 g/dL (79 g/L); white blood cell count, 3.6 × $10^3/\mu L$ (3.6 × 10^9/L) with 16% lymphocytes; and platelet count, 97 × $10^3/\mu L$ (97 × 10^9/L). Serum total-protein level was 4.6 g/dL (46 g/L); albumin, 2.2 g/dL (22 g/L); blood urea nitrogen, 65.1 mg/dL (23.2 mmol/L); and creatinine, 1.4 mg/dL (123.8 μmol/L). Coombs test results were negative. A serological study indicated the presence of antinuclear antibodies with a homogenous pattern (320-fold) and anti–double-stranded DNA antibodies (41.9 U/mL; NR, <12 U/mL). Serum CH50, C3, and C4 levels were low at 27 U/mL (NR, 30 to 50 U/mL), 42 mg/dL (0.42 g/L; NR, 63 to 134 mg/dL [0.63 to 1.34 g/L]), and 11 mg/dL (0.11 g/L; NR, 13 to 36 mg/dL [0.13 to 0.36 g/L)], respectively. Circulating immune complexes were detected by means of the C1q-binding assay (4.6 μg/mL; NR, <3.0 μg/mL). Western blot analysis of serum confirmed immunoglobulin G (IgG) antibodies against HTLV-I antigens (p19, p24, p53, and gp46). HLA haplotypes were A2, A24, B61, B52, DR4, and DR15.

A renal biopsy was performed on December 23, 2004. Light microscopy showed diffuse and global mesangiocapillary proliferation with extensive subendothelial deposits (wire-loop lesions; Fig 1). Immunofluorescence microscopy showed strong granular staining for IgG, IgA, IgM, κ, λ, C3, and C1q in the mesangium and along capillary walls (Fig 2). Renal cryostat sections also were stained with mouse monoclonal IgG to HTLV-I p19 (Chemicon, Temecula, CA) or gp46 (Abcam, Cambridgeshire, UK) and with fluorescein isothiocyanate–conjugated sheep antimouse IgG (ICN/Cappel, Aurora, OH). These HTLV-I antigens were not detected in glomerular lesions. Electron microscopy showed numerous mesangial and subendothelial electron-dense deposits (Fig 3). Virus-like particles were not observed.

SLE was diagnosed based on at least the following findings during the course of disease: renal disorder, hematologic disorder (leukopenia, lymphopenia, and thrombocytopenia), and the presence of antinuclear antibodies and anti–double-stranded DNA antibodies.[10] Glomerulonephritis was classified as active lesions: diffuse global proliferative lupus nephritis (class IV-G [A]) according to the International Society of Nephrology/Renal Pathology Society 2003 classification.[11] Considering the side effects of immunosuppressive agents, he was treated with dipyridamole. From January 26, 2005, he was followed up in a local hospital.

DISCUSSION

Our patient with HAM developed immune complex–mediated glomerulonephritis with wire-loop lesions during long-term follow-up. This case fulfilled at least 4 criteria for the diagnosis of SLE: renal disorder, hematologic disorder, and positive test results for antinuclear antibodies and anti–double-stranded DNA antibodies.[10] The presence of a "full house" of glomerular immunoglobulin and complement deposits supported the diagnosis of lupus nephritis.[11] We therefore considered this a rare case of a patient developing lupus nephritis during the long-term course of HAM.

Fig 1. Light micrograph shows a glomerulus with global involvement of endocapillary and mesangial hypercellularity and matrix expansion with wire-loop lesions. (Periodic acid–Schiff stain; original magnification ×400.)

A potential role for retroviruses as an etiologic factor in SLE has been suggested by the following evidence[4]: (1) the importance of retroviruses in murine lupus models, (2) detection of retrovirus-related antigens and antibodies against retroviral components in organs and sera of patients with SLE, (3) electron microscopic detection of unknown retroviral particles in organs of patients with SLE, (4) the finding that retroviral components can induce immune abnormalities observed in patients with SLE, and (5) the similarity of autoimmune manifestations and immune dysregulation between patients with SLE and those infected with human immunodeficiency virus.

Fig 2. Immunofluorescence microscopy showing strong granular staining for C1q in the mesangium and along capillary walls. (Original magnification ×400.)

Fig 3. Electron microscopy shows electron-dense deposits in the mesangium and along capillary walls. (Lead and uranyl acetate stain.)

Moreover, the development of autoimmunity has been shown in mice transgenic for HTLV-I.[12] It also is known that antinuclear antibodies can be detected in approximately 30% of patients with HAM.[2] Recently, $CD25^+$ cells in the $CD4^+$ population have been shown to have critical roles in the maintenance of self-tolerance by suppressing the activation and expansion of self-reactive T cells that cause autoimmunity.[13] Yamano et al[14] recently showed that $CD4^+$ $CD25^+$

Table 1. Cases of SLE Accompanied by HTLV-I Infection (ATL or HAM)

Reference	Age (y)/Sex	HTLV-I Infection	Occurrence of SLE Before/After ATL/HAM Onset	Lupus Nephritis*
Ito et al[7]	64/M	ATL	At the same time	V
Takayanagui et al[8]	66/F	HAM	>6 y after HAM	
Takayanagui et al[8]	53/F	HAM	>2 y after HAM	
Miura et al[9]	61/F	HAM	14 y before HAM	
Present case	77/M	HAM	16 y after HAM	IV-G (A)

*International Society of Nephrology/Renal Pathology Society 2003 classification.

T cells are the major reservoir of HTLV-I provirus, and functions of these cell populations can be altered in patients with HAM. Their observations suggest that $CD4^+$ $CD25^+$ T cells infected with HTLV-I may lack regulatory T-cell function, leading to the development of autoimmune diseases in HTLV-I–infected patients.

However, to our knowledge, an association between SLE and ATL or HAM has been reported in only 5 cases.[6-9] Clinical features of the reported cases and our case are listed in Table 1 (1 patient with HAM[6] is not included in Table 1 because detailed clinical information was not described). Median age of these patients was 64 years (range, 53 to 77 years). Two patients were men and 3 patients were women. One patient with ATL developed SLE simultaneously; membranous lupus nephritis was shown by a renal biopsy. Three of the remaining 4 patients, including our patient, presented with HAM during 2 to 14 years before the occurrence of SLE. Conversely, 1 patient had a 14-year history of SLE before the onset of HAM. In these patients with HAM, the development of glomerulonephritis was shown in only our patient. A renal biopsy showed typical morphological changes of lupus nephritis class IV-G (A), the endothelial pattern of immune complex–mediated injury.[11] In our patient, we were unable to detect HTLV-I antigens or virus-like particles in glomerular lesions. It therefore is unlikely that HTLV-I antigen-antibody immune complexes occurred in the kidney of our patient.

The rarity of the association between SLE and ATL or HAM raises questions of whether it may be a mere coincidence, SLE may be related to HTLV-I infection, or several systemic manifestations of HLTV-I infection may mimic SLE by the criteria for its diagnosis.[15] It is well known that SLE affects mostly women of childbearing age.[16] Conversely, all reported patients with SLE with ATL or HAM were middle aged or elderly, as discussed, suggesting that the development of SLE in these patients may be associated with underlying disorders. Our patient developed SLE and immune complex–mediated glomerulonephritis during the long-term course of HAM. Thus, additional studies including long-term follow-up investigations of patients with HAM are needed to explore a possible link between SLE and HTLV-I infection.

REFERENCES

1. Popovic M, Reitz MS Jr, Sarngadharan MG, et al: The virus of Japanese adult T-cell leukaemia is a member of the human T-cell leukaemia virus group. Nature 300:63-66, 1982

2. Nakagawa M, Izumo S, Ijichi S, et al: HTLV-I-associated myelopathy: Analysis of 213 patients based on clinical features and laboratory findings. J Neurovirol 1:50-61, 1995

3. Barmak K, Harhaj E, Grant C, Alefantis T, Wigdahl B: Human T cell leukemia virus type I-induced disease: Pathways to cancer and neurodegeneration. Virology 308:1-12, 2003

4. Sekigawa I, Ogasawara H, Kaneko H, Hishikawa T, Hashimoto H: Retroviruses and autoimmunity. Intern Med 40:80-86, 2001

5. Adelman MK, Marchalonis JJ: Endogenous retroviruses in systemic lupus erythematosus: Candidate lupus viruses. Clin Immunol 102:107-116, 2002

6. Vernant JC, Buisson GG, Sobesky G, Arfi S, Gervaise G, Román GC: Can HTLV-1 lead to immunological disease? Lancet 2:404, 1987 (letter)

7. Ito H, Harada R, Uchida Y, et al: Lupus nephritis with adult T cell leukemia. Nephron 55:325-328, 1990

8. Takayanagui OM, Moura LS, Petean FC, Bíscaro TA, Covas DT, Osame M: Human T-lymphotropic virus type I-associated myelopathy/tropical spastic paraparesis and systemic lupus erythematosus. Neurology 48:1469-1470, 1997

9. Miura T, Tanaka H, Makino Y, et al: Human T cell leukemia virus type I-associated myelopathy in a patient with systemic lupus erythematosus. Intern Med 38:512-515, 1999

10. Hochberg MC: Updating the American College of Rheumatology revised criteria for the classification of systemic lupus erythematosus. Arthritis Rheum 40:1725, 1997 (letter)

11. Weening JJ, D'Agati VD, Schwartz MM, et al: The classification of glomerulonephritis in systemic lupus erythematosus revisited. Kidney Int 65:521-530, 2004

12. Iwakura Y, Saijo S, Kioka Y, et al: Autoimmunity induction by human T cell leukemia virus type 1 in transgenic mice that develop chronic inflammatory arthropathy resembling rheumatoid arthritis in humans. J Immunol 155: 1588-1598, 1995

13. Sakaguchi S, Sakaguchi N, Shimuzu J, et al: Immunologic tolerance maintained by $CD25^+$ $CD4^+$ regulatory T cells: Their common role in controlling autoimmunity, tumor immunity, and transplantation tolerance. Immunol Rev 182:18-32, 2001

14. Yamano Y, Cohen CJ, Takenouchi N, et al: Increased expression of human T lymphocyte virus type I (HTLV-I) Tax11-19 peptide-human histocompatibility leukocyte antigen A*201 complexes on $CD4^+$ $CD25^+$ T cells detected by peptide-specific, major histocompatibility complex-restricted antibodies in patients with HTLV-I-associated neurologic disease. J Exp Med 199:1367-1377, 2004

15. Ijichi S, Osame M: Human T-cell lymphotropic virus type I and systemic lupus erythematosus. Intern Med 38:459-460, 1999

16. Mok CC, Lau CS: Pathogenesis of systemic lupus erythematosus. J Clin Pathol 56:481-490, 2003

Available online at www.sciencedirect.com
SCIENCE DIRECT
ELSEVIER
Biochemical and Biophysical Research Communications 338 (2005) 1845–1852
BBRC
www.elsevier.com/locate/ybbrc

KL-6, a human MUC1 mucin, promotes proliferation and survival of lung fibroblasts

Shinichiro Ohshimo [a], Akihito Yokoyama [a,*], Noboru Hattori [a], Nobuhisa Ishikawa [a], Yutaka Hirasawa [b], Nobuoki Kohno [a]

[a] *Department of Molecular and Internal Medicine, Division of Clinical Medical Science, Programs for Applied Biomedicine, Graduate School of Biomedical Sciences, Hiroshima University, Hiroshima, Japan*
[b] *Department of Respiratory Medicine, Kitaishikai Uchiyama Hospital, Ehime, Japan*

Received 18 October 2005
Available online 2 November 2005

Abstract

The serum level of KL-6, a MUC1 mucin, is a clinically useful marker for various interstitial lung diseases. Previous studies demonstrated that KL-6 promotes chemotaxis of human fibroblasts. However, the pathophysiological role of KL-6 remains poorly understood. Here, we further investigate the functional aspects of KL-6 in proliferation and apoptosis of lung fibroblasts. KL-6 accelerated the proliferation and inhibited the apoptosis of all human lung fibroblasts examined. An anti-KL-6 monoclonal antibody counteracted both of these effects induced by KL-6 on human lung fibroblasts. The pro-fibroproliferative and anti-apoptotic effects of KL-6 are greater than and additive to those of the maximum effective concentrations of platelet-derived growth factor, basic fibroblast growth factor, and transforming growth factor-β. These findings indicate that increased levels of KL-6 in the epithelial lining fluid may stimulate fibrotic processes in interstitial lung diseases and raise the possibility of applying an anti-KL-6 antibody to treat interstitial lung diseases.

Keywords: Interstitial lung disease; Idiopathic pulmonary fibrosis; Therapeutic agent; Apoptosis

Interstitial lung diseases (ILD), including idiopathic pulmonary fibrosis (IPF), are a diverse group of pulmonary disorders characterized by alveolitis and intra-alveolar fibrosis [1]. A number of ILD have known etiologies, such as infection, collagen vascular diseases, exposure to environmental dusts, drugs, and radiation. However, the etiology of IPF remains unknown. Recent studies have suggested that IPF is primarily an epithelial/fibroblastic, rather than inflammatory disorder [2]. Despite recent progress in understanding the pathogenesis of IPF, the precise molecular mechanisms leading to IPF remain unclear.

We have previously identified a mouse IgG_1 monoclonal antibody (mAb) that recognizes a protein with a sialylated sugar chain, KL-6 [3]. KL-6 is a high molecular weight glycoprotein that is expressed on the apical borders of normal secretary alveolar epithelial cells (AEC) and is classified as a transmembrane MUC1 mucin [4]. We have been extensively investigating the relationship between KL-6 and ILD. We found that the serum level of KL-6 is a clinically useful marker for various ILD [5–8], including IPF [9], collagen vascular disease-associated interstitial pneumonitis, radiation pneumonitis [10], drug-induced pneumonitis [11], hypersensitivity pneumonitis, pulmonary sarcoidosis [12], pulmonary alveolar proteinosis [13], acute respiratory distress syndrome [14], and *Pneumocystis carinii* pneumonia [15]. Our previous study demonstrated that a reduction in the serum KL-6 level 1 week after the corticosteroid therapy is an early predictor for favorable outcomes for patients with IPF [9], and this suggests that the serum KL-6 level is a prognostic factor for ILD patients. On the basis of these studies, the serum level of KL-6 has been approved by Japan's health insurance program as a

* Corresponding author. Fax: +81 82 255 7360.
E-mail address: yokoyan@hiroshima-u.ac.jp (A. Yokoyama).

0006-291X/$ - see front matter © 2005 Elsevier Inc. All rights reserved.
doi:10.1016/j.bbrc.2005.10.144

diagnostic marker for ILD and more than 800,000 patients are now examined per year.

Despite the clinical importance of KL-6, however, the pathophysiological role of KL-6 in ILD remains poorly elucidated, except for its chemotactic effect on normal human lung fibroblasts [16]. The level of KL-6 in BALF is almost comparable with those in circulating blood, indicating that an extremely large quantity of KL-6 exists in the epithelial lining fluid (ELF) of patients with ILD. Therefore, we hypothesized that the abundant KL-6 in ELF might be involved in the pathogenesis of ILD. To extend our investigations of the interactions between KL-6 and fibroblasts, we attempted to elucidate whether KL-6 affects the proliferation and/or apoptosis of human lung fibroblasts.

Materials and methods

Materials and reagents. The reagents used in the present study were obtained as follows: Eagle's minimum essential medium-α (MEM-α) was obtained from Nikken BioMed., Kyoto, Japan; paraformaldehyde, Triton X-100 and Hoechst 33342 were from Sigma–Aldrich, St. Louis, MO, USA; the CellTiter 96 AQueous One Solution Cell Proliferation Assay kit using 3-(4,5-dimethylthiazol-2-yl)-5-(3-carboxymethoxyphenyl)-2-(4-sulfophenyl)-2H-tetrazolium (MTS) was from Promega, Madison, WI, USA; the Cell Proliferation ELISA kit using bromodeoxyuridine (BrdU) and the In Situ Cell Death Detection kit POD were from Roche Diagnostics, Mannheim, Germany; Diff-Quik was from Sysmex, Kobe, Japan; anti-Fas mAb (CH-11) was from Medical and Biological Laboratories, Nagoya, Japan; cycloheximide was from BIOMOL Research Lab., PA, USA; platelet-derived growth factor-BB (PDGF-BB) was from Becton Dickinson Lab., Bedford, MA, USA; recombinant human transforming growth factor (TGF)-β_1, -β_2, and recombinant human basic-fibroblast growth factor (bFGF) were from R&D Systems, Minneapolis, MN, USA; the immunoaffinity column (cyanogen bromide-activated Sepharose 4B) was from GE Healthcare, Amersham Biosciences, Uppsala, Sweden; flat-bottomed 96-well plates were from Sumitomo Pharm. Lab., Tokyo, Japan; eight-well chamber slides were from Nalge Nunc International, Rochester, NY, USA.

Cell culture. Human lung fibroblast lines CCD-11Lu, CCD-13Lu, CCD-16Lu, and CCD-18Lu were obtained from the American Type Culture Collection (Manassas, VA, USA). Human lung fibroblast lines WI-38, MRC-5, and MRC-9; a mouse lung fibroblast line NIH3T3, and a mouse skin fibroblast line A-9 were obtained from the Japanese Cancer Research Resources Bank (Tokyo, Japan). The cells were cultured in MEM-α supplemented with 10% heat-inactivated fetal calf serum, 100 U/ml penicillin, and 100 μg/ml streptomycin at 37 °C in 5% CO_2. Cells taken between the 3rd and the 5th passages were used for the experiments.

Purification of anti-KL-6 monoclonal antibody. The anti-KL-6 mouse IgG_1 monoclonal antibody (mAb) was purified by use of a protein A affinity column (Affi Gel Protein A MAPS II Kit; Bio-Rad, Hercules, CA, USA) from ascites collected from the mice bearing an anti-KL-6 mAb-producing hybridoma according to the manufacturer's protocol.

Purification of KL-6. KL-6 was purified from the culture supernatant of a human breast cancer cell line YMB-S, which was established in our laboratory [17]. In brief, the culture supernatant was mixed with starting buffer (0.01 M Tris–HCl buffer, pH 7.5, containing 0.15 M NaCl and 0.1% NaN_3) and centrifuged at 12,000 rpm for 20 min. The resulting supernatant was applied to a KL-6 immunoaffinity column equilibrated with 10 column volumes of starting buffer. The molecules retained on the column were eluted with 0.01 M KPO_4 (pH 2.0) containing 4 M $MgCl_2$ and neutralized with 1 M Tris–HCl buffer (pH 8.0). The concentration of protein and KL-6 in each fraction was measured and the fractions showing high KL-6 levels were collected and dialyzed against starting buffer at 4 °C for 18 h. The dialyzed sample was lyophilized and then dissolved in 2 ml of distilled water.

Determination of KL-6 concentration. The concentration of KL-6 was measured by a sandwich-type electrochemiluminescence immunoassay (ECLIA) using an ORIGEN Analyzer (IGEN, Gaithersburg, MD, USA) according to the manufacturer's protocol. In brief, the KL-6 solution was incubated with anti-KL-6 antibody-coated magnetic beads and the beads were then separated by use of a magnetic rack. Ruthenium-labeled anti-KL-6 antibody was added to the beads as a second antibody following a wash with PBS. The reaction mixture was placed into the electrode and the photons emitted from the Ruthenium were measured with a photomultiplier.

Assessment of cell proliferation. The proliferative activity of fibroblasts was quantified with a CellTiter 96 AQueous One Solution Cell Proliferation Assay kit using MTS according to the manufacturer's protocol. In brief, 1×10^4 cells were seeded into flat-bottomed 96-well plates and cultured in the presence of various concentrations of KL-6 for 48 h. Twenty microliters of MTS reagent was added to each well and wells were incubated for 1 h at 37 °C in 5% CO_2. The absorbance at 490 nm was recorded with a Model-550 ELISA plate reader (Bio-Rad, Hercules, CA, USA). The absorbance values were divided by values obtained from cells cultured in the absence of KL-6, and each resulting value was designated a promotion index. In the experiments to examine the effect of the anti-KL-6 mAb, the proliferative activity of fibroblasts in medium containing 100 U/ml of KL-6 and various concentrations of anti-KL-6 mAb (0–100 μg/ml) was assessed.

Measurement of DNA synthesis. The rate of DNA synthesis in CCD-11Lu was measured with a Cell Proliferation ELISA kit using BrdU according to the manufacturer's protocol. In brief, 1×10^4 cells were seeded in the presence of 100 U/ml of KL-6 for 48 h and were then incubated for another 2 h after addition of 10 μmol/L of BrdU. The cells were then denatured with denaturing solution and incubated for 90 min with 0.075 U/ml of mouse anti-BrdU mAbs conjugated to peroxidase. After removing the antibody conjugates, substrate solution was added and the reaction was stopped after 10 min by the addition of a 2 M HCl solution. The absorbance at 450 nm was recorded with a Model-550 ELISA plate reader.

Assessment of cell apoptosis. Apoptotic cells were morphologically evaluated using Diff-Quik or 10 μM Hoechst 33342 according to the manufacturer's protocol. Quantification of surviving cells following induction of apoptosis was performed using a CellTiter 96 AQueous One Solution Cell Proliferation Assay kit. In brief, 1.5×10^4 cells were seeded into flat-bottomed 96-well plates and cultured for 24 h. After removing the culture medium, the cells were incubated with fresh media containing 100 ng/ml of anti-Fas mAb (CH-11) and 10 μg/ml of cycloheximide in the presence or absence of KL-6. After an additional 12 h of incubation, the viable cells were quantified using the kit according to the manufacturer's protocol. To examine the effect of anti-KL-6 mAb, the cells were incubated in medium containing anti-Fas mAb (100 ng/ml), cycloheximide (10 μg/ml), and KL-6 (100 U/ml) in the presence of various amounts of anti-KL-6 mAb (0–100 μg/ml). After 12 h of incubation, apoptotic cells were quantified using the methods described above.

DNA fragmentation of apoptotic cells was also assessed using the terminal transferase dUTP nick-end labeling (TUNEL) assay. Fragmented DNA was detected with an In Situ Cell Death Detection kit POD following the manufacturer's protocol. In brief, 1.5×10^4 cells were cultured for 24 h and apoptosis was induced by anti-Fas mAb and cycloheximide on eight-well chamber slides. The cells were fixed with 4% paraformaldehyde for 30 min at room temperature and then permeabilized with 0.1% Triton X-100 in 0.1% sodium citrate on ice for 2 min. Fifty microliters of TUNEL reaction buffer was placed onto the slides, which were then incubated at 37 °C for 1 h. The percentage of TUNEL positive cells relative to the total cells was calculated.

Comparison of the pro-proliferative and anti-apoptotic effect of bFGF, PDGF-BB, TGF-β_1, and -β_2, with that of KL-6. In brief, 1×10^4 cells were seeded into flat-bottomed 96-well plates and cultured in the presence of bFGF (100 ng/ml), PDGF-BB (20 ng/ml), TGF-β_1, and -β_2 (2 ng/ml) and KL-6 (100 and 1000 U/ml) for 48 h. The proliferative activity of fibroblasts was quantified with MTS reagent as described above. We have